EJN European Journal of Neuroscience

FENS Federation of European Neuroscience Societies

European Journal of Neuroscience, pp. 1–12, 2016 doi:10.1111/ejn.13496

Parallel activation of prospective motor plans during visually-guided sequential saccades

Neha Bhutani,[1] Sonal Sengupta,[2] Debaleena Basu,[2] Nikhil G. Prabhu[2] and Aditya Murthy[2]
[1]National Brain Research Centre, Manesar, Haryana, India
[2]Centre for Neuroscience, Indian Institute of Science, Bangalore, 560012 Karnataka, India

Keywords: adaptation, midway saccades, motor planning, sequential saccades

Edited by John Foxe
Received 2 April 2016, revised 1 December 2016, accepted 2 December 2016

Abstract

Behavioural evidences suggest that sequential saccades to multiple stimuli are planned in parallel. However, it remains unclear whether such parallel programming reflects concurrent processing of goals or whether multiple motor plans coexist, unfolding subsequently during execution. Here we use midway saccades, directed at intermediate locations between two targets, as a probe to address this question in a novel double-step adaptation task. The task consisted of trials where subjects had to follow the appearance of two targets presented in succession with two sequential saccades. In some trials, the second target predictably jumped to a new location during the second saccade. Initially, the second saccade was aimed at the final target's location before the jump. As subjects adapted to the target jump, saccades were aimed to the second target's new location. We tested whether the spatial distribution of midway saccades could be explained as an interaction between two concurrent saccade goals, each directed at the two target locations, or between the initial motor plan to the first target location and a prospective motor plan directed from the initial to the final target location. A shift in the midway saccades' distribution towards the jumped location of the second target following adaptation indicated that the brain can make use of prospective motor plans to guide sequential eye movements. Furthermore, we observed that the spatiotemporal pattern of endpoints of midway saccades can be well explained by a motor addition model. These results provide strong evidence of parallel activation of prospective motor plans during sequential saccades.

Introduction

Complex actions are thought to be parsed into sequences of simpler elements that are represented in the brain well before the action begins (Lashley, 1951; Keele, 1968). Behavioural evidence supporting this view derives from errors of ordering in which the element to be executed is sometimes substituted by the next element in the sequence (Verwey, 1995; Page & Norris, 1998). Neurophysiological evidence for preplanning of movement sequences comes from the findings of concurrent representations of impending sequential movements in the neurons of different cortical regions (Barone & Joseph, 1989; Funahashi *et al.*, 1997; Averbeck *et al.*, 2002; Mushiake *et al.*, 2006).

Vision also requires making sequential saccadic eye movements to foveate different parts of a scene. Evidence for parallel programming of sequential saccades comes from behavioural studies using double-step tasks where a target steps to a new location while the saccade to the first target was still in preparation(Becker & Jürgens, 1979; McPeek *et al.*, 2000; Ray *et al.*, 2004; Sharika *et al.*, 2008). More specifically, it is now established that the intersaccade interval (ISI) between the two saccades decreases with increase in the interval between the appearance of the second target and the first saccade onset in the sequence, which is the time available to programme the second saccade while the first is still being processed (called the reprocessing time or RPT). Sometimes, the ISI may even fall below the normal reaction time (Goossens & Van Opstal, 1997; McPeek & Keller, 2001). Thus parallel programming allows faster execution of movement sequences. However, parallel saccade plans may interact to produce erroneous midway saccades that land at an intermediate location between the locations of the two sequential targets (Findlay, 1982; Viviani and Swensson, 1982; Coëffé and O'Regan, 1987; Zambarbieri *et al.*, 1987; Bhutani *et al.*, 2012, 2013). Therefore, understanding how midway saccades are produced can provide insight into the nature of representations that are held in abeyance while sequential movements unfold in real time.

Various neurophysiological studies have revealed that saccade generation involves a continuum of stages ranging from visual encoding of targets, goal selection and saccade motor planning (Thompson *et al.*, 1996).These three stages have been schematized in Fig. 3 to define them and illustrate the differences between them. Typically, in standard visuomotor tasks the location of the target (bottom up signal) is indistinguishable from the goal (top down

Correspondence: Dr. Aditya Murthy, as above.
E-mail: aditya@cns.iisc.ernet.in

signal) but can be distinguished when the sensory to motor map is altered. For example, for an antisaccade, the goal location is opposite to the bottom up sensory signal. Likewise, the difference between a goal location and a motor plan is typically indistinguishable in single saccades but can be dissociated by having the saccade goal step to a new location during the execution of the saccade. Gradually over time, the oculomotor system compensates or adapts to the target step by changing the gain of the motor command that is thought to involve the cerebellum downstream of the structures where the location of the goal is encoded, at least for reactive saccades (Frens & Van Opstal, 1997; Hopp & Fuchs, 2004; Cotti *et al.*, 2009).

In the context of these distinct representations, midway saccades may be a consequence of interactions occurring in any of these stages. Although, in principle, the contributions of sensory- and movement-based representations can and have been tested (Robinson & Fuchs, 1969; Glimcher & Sparks, 1993; Schiller & Sandell, 1983; Van Opstal & Van Gisbergen, 1990; Edelman & Keller, 1998), the interpretations of these experiments are rendered difficult since in many cells of the oculomotor system, the activity reflecting sensory, goal and motor representations are typically multiplexed and hard to disambiguate (Bruce & Goldberg, 1985; Shen & Paré, 2007). Interpreting the results from microstimulation experiments is also limited by the inability of microstimulation to selectively activate sensory, goal or movement representations (Armstrong *et al.*, 2006; Histed *et al.*, 2009).

In a previous paper (Bhutani *et al.*, 2012), we used a direct behavioural readout using different versions of a double-step task that required multiple movement plans to show that midway saccades can be generated as a consequence of the interaction of two saccade plans in stages downstream to sensory processing. The task-specific increase in the midway saccades in Parkinson's disease subjects and basal ganglia inactivated monkeys provided further evidence to support this finding (Bhutani *et al.*, 2013). While these results rule out a sensory-based account of saccade averaging, it remains unclear whether midway saccades are produced as a result of the interaction of concurrent saccade goals or as a result of the interaction of parallel motor plans. Here, we used the spatial spread of the endpoint of midway saccades to test for the interaction of concurrent motor plans by using an adaptation task to manipulate the motor stage of the second saccade without altering the second saccade goal. Thus, any change observed in the midway saccades' scatter could be attributed to the interaction of motor stages. We further tested the validity of these results by using a collicular vector addition model (Van Gisbergen *et al.*, 1987b; Goossens & Van Opstal, 2006) for its ability to explain the spatiotemporal pattern of midway saccades to ascertain the nature of these interactions.

Methods

Subjects

Data from sixteen naïve human subjects are presented in this study. Eight subjects (6 males and 2 females; ages ranging between 21 and 31 years) performed the *adaptation* task, whereas the other eight (5 males and 3 females; ages ranging between 21 and 31 years) performed the *different eccentricity* task. All subjects gave their informed consent in accordance with the institutional human ethics committee of the Indian Institute of Science (IISc), that reviewed and approved the protocol. The adaptation data consisted of approximately 500 trials. For the different eccentricity task, data were collected from each subject in three sessions each of approximately 500 trials. Subjects were given verbal instructions and 50–100 practice trials before each session. Correct trials were followed by an auditory beep to provide feedback to subjects. All subjects were monetarily rewarded for their performance.

Adaptation task

The double-step adaptation task (Fig. 1) is a modification of the FOLLOW task (Ray *et al.*, 2004) and is divided into three blocks (Fig. 1a): pre-adaptation (100–150 trials), adaptation (~250 trials) and post-adaptation (100–150 trials). Each block consisted of two types of trials–no-step (40%) and step (60%), that were pseudo-randomly interleaved. Each trial started with the appearance of a central fixation point (FP), which was a 1° white square, presented on a dark background. Subjects had to fix their gaze within a ± 2.5° electronic window centred at the FP. On no-step trials, following a random fixation duration of 300–800 ms, the FP disappeared and an initial green saccade target (IT; 1° × 1°) appeared at either the location 1 or 2 (i.e. 2 = top-left and 1 = top-right respectively) at an eccentricity of 12° and subtending an angle of 45° with respect to the vertical meridian. Subjects were instructed to saccade to the green target on its appearance. No-step trials were identical across the three blocks. Step trials were identical in the pre- and post-adaptation blocks (Fig. 1c), where following the appearance of the initial green target (IT; 1° × 1°) at location 2, a final red target (FT; 1° × 1°) would appear at location 1 after a fixed temporal delay called the Target Step Delay (TSD) of ~16 ms. The angular separation between the two targets was 90°. Subjects had to follow the sequence of appearance of the two targets with two successive saccades. On the step trials of the adaptation block, the red target shifted to a new location (FT-new) during the second saccade (grand average of ~35 ms after the second saccade onset; Table 1; Fig. 1d). However, this occurred only on those trials where subjects had made a correct saccade to the initial target. The start of the second saccade was determined by setting an online velocity threshold criterion of 30°/s.

If subjects fixated the targets within ±2.5°, the trials were counted as successful and were accompanied by an auditory beep to provide feedback to the subjects. Subjects were not told about the target shift. Thus, to keep them motivated during the task, the feedback beep on step trials was provided if the subject made a second saccade to the old or the new location of the second target. The targets remained on throughout the trial duration.

Different eccentricity double-step task

Another group of eight naïve subjects performed a second version of the double-step FOLLOW task. Here 60% of the trials were no-step trials. However, the no-step target or the initial target in step trials could appear at any of eight equidistant locations on an imaginary circle of radius 12° from the FP. An angular separation of 45° was maintained between the IT and FT locations. On a random half of the step trials, the FT appeared at the same eccentricity as the IT (i.e. at 12°), whereas on the remaining trials the FT appeared at a reduced eccentricity of 6°. The targets remained on throughout the trial. Five target step delays (TSDs) that ranged between 16 and 150 ms and accurate to the screen refresh rate were used. Variable TSDs allowed control over the reprocessing time (RPT), which is the time between the appearance of the onset of first saccade and the appearance of the final target. In general shorter RPTs were associated with longer TSDs and vice versa. The instructions were same as in the pre-adaptation or post-adaptation block of the adaptation task.

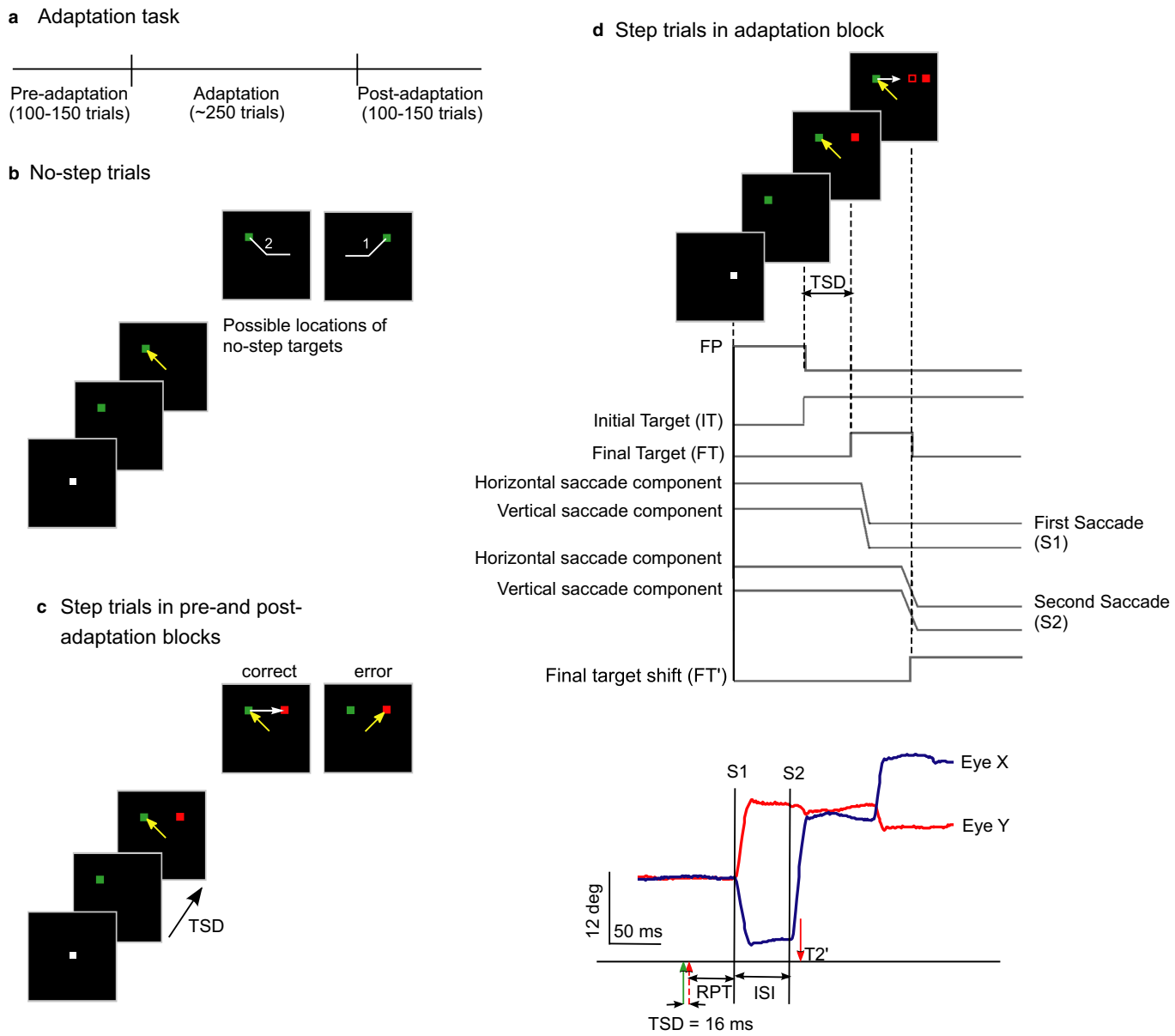

FIG. 1. Double-step adaptation task. (a) The task was divided into three blocks, *pre-adaptation*, *adaptation* and *post-adaptation* blocks. Each block consisted of *no-step* (40%) and *step* (60%) trials that were pseudo-randomly interleaved. (b) Spatial and temporal sequence of events in no-step trials. (c) On step trials in the pre- and post- adaptation blocks, the location of the Initial Target (IT) and the Final Target (FT) was always fixed. The FT appeared at a Target Step Delay (TSD) of 16 ms after the IT. Subjects had to follow the sequence of appearance of two targets with two saccades. A saccade directly to the second target was considered an error. (d) Temporal sequence of events in an adaptation step trial. Following fixation, the initial green target and the final red target were presented just as in the pre-adaptation block. During the execution of the second saccade (white arrow), the final target (open red square) disappeared from its original location and shifted 8° to its right (FT-new; red filed square). Starting from the beginning of the trial (denoted by a solid, black vertical line), grey lines indicate (by means of a jump from baseline in the respective horizontal trace), the appearance of the fixation box, initial target, final target, horizontal and vertical components of the first (S1) and second (S2) saccades, and shift of the final target during the second saccade. *(Lower)* The timeline for the shift of the final target with respect to the two saccades in a typical trial is shown. Blue and red lines represent the horizontal (EyeX) and vertical (EyeY) eye position, respectively. Solid green, dashed red and solid red arrows represent the time of appearance of the IT, FT and the shifted FT. Black lines represent the onset of first (S1) and second (S2) saccades.

Recording set up

Experiments were computer-controlled using TEMPO/VDEOSYNC software (Reflective Computing, St. Louis, MI, USA) that displayed visual stimuli, sampled and stored eye position and other behavioural parameters. Eye position was sampled at 240 Hz using an infrared pupil tracker (ISCAN, Boston, MA, USA) that interfaced with TEMPO software in real time. Before starting the recording session, each subject was made to look at 5 positions on the monitor; one at fixation in the centre of the monitor and 4 (horizontal left, right; vertical up, down) target positions. The monitor (SONY Bravia LCD monitor; 42 inch; 60 Hz refresh rate; 640 × 480 resolution) was placed 57 cm from the subject. While subjects fixated the targets, we adjusted the horizontal and vertical gain parameters in real time, such that the endpoint of saccades would typically coincide with the centre of the electronic windows centred on their respective target positions (but visible only to the

TABLE 1. Mean ± SEM for second target shifts following the onset of second saccades in step trials of the adaptation blocks for all subjects

Subject	2nd target shift w.r.t. second saccade onset (mean ± SEM) ms
AR	38.72 ± 0.62
JA	32.19 ± 0.35
NI	37.83 ± 0.15
NP	39.29 ± 0.09
NT	32.44 ± 0.21
PS	36.07 ± 0.13
SD	31.72 ± 0.12
ST	31.98 ± 0.06

experimenter). Since the electronic window (for fixation and target position) was displayed throughout the experiment we could adjust the gains and recalibrate the fixation point from time to time to compensate for drifts and slight changes in head positions. Furthermore, to facilitate calibration across trials, each trial began only after subjects' eye position was deemed to be within the limits set by the fixation window ± 2.5°. Since the targets were displayed at either 6° or 12° of eccentricity with a minimum angular separation between the two targets in a step trial as 45°, the minimum spatial separation between two targets was ~8°. Thus, the error introduced as a consequence of our calibration procedure (± 2.5°) and the typical accuracy of the tracker (~1°) was well within limits to be confident that trials were correctly classified.

Data analyses

All offline analyses were performed using custom made programs written in MATLAB (Mathworks, USA). The analogue eye position data were smoothed and blinks were removed. A velocity threshold of 30°/sec was used to mark the initiation of saccades. The saccade detection algorithm was subsequently verified manually. All blink-perturbed saccades were eliminated from the analyses. Trials in which saccade latency was <80 ms (anticipatory saccades) were rejected. All statistical tests were done using the Statistical toolbox in MATLAB. Normality in each condition was tested using the Lilliefors test. For non-normal data sets, non-parametric versions of these tests were used. Unless mentioned otherwise, all the results of averaged data are presented as 'mean ± SEM.'

Midway saccades

Saccades that landed at an intermediate location between the initial and final targets were called midway saccades. To quantify the occurrence of midway saccades, we first calculated the 95% confidence interval for the direction of endpoint scatter of correct no-step saccades for each target location (Fig. 2). Those step trials, where the initial saccade landed between the locations of IT and FT, but beyond the 95% confidence interval of the distribution of no-step saccade endpoints to the two targets, were called midway saccades (Bhutani *et al.*, 2012; Fig. 2).We observed 17.34 ± 2.83% of midway saccades in the adaptation task and 19.24 ± 1.68% of midway saccades in the different eccentricity task.

Model simulations

The endpoint scatter of initial saccades in the step trials was modelled as a function of the reprocessing time (RPT), which is the time during which the two saccades are planned in parallel. For this we

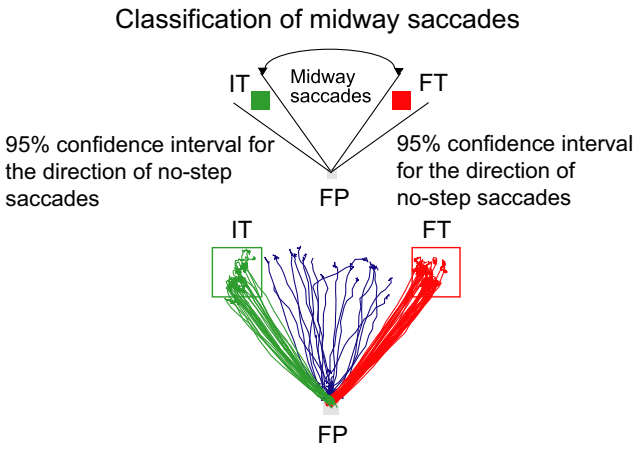

FIG. 2. Classification of midway saccades. The initial saccades in step trials that landed between the locations of IT (green traces) and FT (red traces) but beyond the 95% confidence interval of the distribution of correct no-step saccade endpoints to the two targets are considered midway saccades (blue traces). FP is the fixation point.

simulated the values of RPT using the framework of a LATER model (Linear Accumulation to Threshold with Ergodic Rate; Carpenter & Williams, 1995; Reddi & Carpenter, 2000), which is a ramp-to-threshold model of reaction time and has been successful in explaining the reaction time (RT) distribution of single saccades. In the LATER model, a GO process representing the preparatory activity for a saccade is initiated following stimulus presentation; and a saccade is triggered once the build-up activity in the GO process reaches the threshold. The accumulation was determined by the following equation:

$$a_{GO,t} = \mu_{GO} \times t \quad (1)$$

where $a_{GO,t}$ represented the activity in the accumulator at time t. The mean growth rate of the GO unit is given by μ_{GO}, which varied stochastically from trial to trial.

No-step trials

The parameters describing the GO accumulator were randomly selected from a distribution with mean μ_{GO} and standard deviation σ_{GO}. The rates of the GO process were allowed to vary across trials, but the accumulation of build-up activity at every time-step was kept constant. On each trial, the accumulation ($a_{GO,\ t}$) started after a constant delay τ of 60 ms. This value of τ was set to approximate the average latency of visual cells in the macaque visuomotor system (Schmolesky *et al.*, 1998; Pouget *et al.*, 2005). Since the target was presented throughout the trial duration, there was no time limit on the accumulation of build-up activity. Once the activity reached the threshold, which was arbitrarily set to a value of 1, a saccade was triggered. Thus, the time taken for the activity to hit the threshold from the time of target onset was the reaction time (RT_{GO}) of the saccade for that trial. For each subject, 2000 no-step trials were simulated to obtain the RT_{GO} distribution. The simulated RT_{GO} distribution was then compared with the observed no-step RT distribution by minimizing the Kolmogorov-Smirnov (Massey, 1951) statistic in the parameter space (μ_{GO} and σ_{GO}), which gave the maximum absolute deviation between the cumulative probability distribution of experimentally observed no-step RTs and predicted RTs. This procedure was repeated 1000 times, using different sets of random initial parameter values. The best parameter sets were obtained individually for each subject.

Step trials

On step trials, a single GO process representing the first saccade was simulated using parameters from the corresponding no-step RT (μ_{GO} and σ_{GO}) simulations. Similar to no-step trials, the accumulation of the GO1 $(a_{GO1,t})$ process started after a visual delay (τ) of 60 ms following the initial target presentation. For each trial, the TSD was chosen randomly from the set of TSDs used in the experiment. In total, 5000 step trials were simulated for each subject. The time at which the activity hit the threshold (simulated RT) was given by RT_{GO1} and respectively. The simulated value of RPT (reprocessing time), RPT_{sim}, for each trial, which denotes the time interval between the onset of the target step and the first saccade reaction time was then obtained as:

$$RPT_{sim} = RT_{GO1} - TSD \tag{2}$$

Goodness of fit

The goodness of fit, R^2, was used to compare the two models. R^2 was given by the following equation:

$$R^2 = 1 - \left(\frac{SS_{err}}{SS_{total}}\right) \tag{3}$$

where, SS_{err}, or the residual sum of squares was defined as:

$$SS_{err} = \sum_i^n (Y_i - F_i)^2 \tag{4}$$

and SS_{total}, or the total sum of squares was defined as:

$$SS_{total} = \sum_i^n (Y_i - \bar{Y})^2 \tag{5}$$

In the above equations $\bar{Y}$ represented mean of the observed saccade endpoints and was given as:

$$\bar{Y} = \sum_i^{n=10} \frac{Y_i}{10} \tag{6}$$

where, the relative distance Y_i and F_i were calculated as a difference between the observed and predicted mean endpoints for the ith RPT bin from the IT location [0°, 12°].

$$Y_i = \sqrt{\left(H_{i,obs}{}^2 + V_{i,obs}{}^2\right)} \tag{7}$$

$$F_i = \sqrt{\left(H_{i,pred}{}^2 + V_{i,pred}{}^2\right)} \tag{8}$$

H_i and Vi represent the observed (7) and predicted (8) shift in the horizontal and vertical components of endpoints of saccades in the ith RPT bin from the IT location [0°, 12°] in step trials. Ideally, the value of R^2 ranges between 0 and 1. However, since in this study the predictions were not based on a model-fitting procedure, R^2 values could be less than zero.

Results

Selectively adapting the second saccade in a double-step FOLLOW task, provided an opportunity to test the nature of representations during parallel programming since the distinction between sensory, goal and motor stages can be made explicit, as shown in Fig. 3 (see also Quaia *et al.*, 2010). The location of targets, with respect to the fovea or the current fixation point (FP), in visual space can be described by 2D visual vectors, $\overrightarrow{V1}$ and $\overrightarrow{V2}$, which specify where the images of the targets fall on the retina, relative to the fovea that maps onto the current fixation point. Since in the FOLLOW task, the two targets are behaviourally relevant, they also represent goals $\overrightarrow{G1}$ and $\overrightarrow{G2}$, with $\overrightarrow{G2}$ being defined as the vector from the initial target (IT) to the final target (FT). Movement vectors are represented as $\overrightarrow{M1}$ and $\overrightarrow{M2}$. The motor vector $\overrightarrow{M1}$, which is identical to $\overrightarrow{V1}$ and $\overrightarrow{G1}$, represents the motor plan of the first saccade. Since the subjects are required to follow the appearance of the two targets with sequential saccades, the second movement vector $\overrightarrow{M2}$ is the saccade directed from the IT to final target (FT) and is normally indistinguishable from $\overrightarrow{G2}$. However, following forward adaptation (right panel), the goal of the second saccade is unaltered, whereas the gain of the second saccade vector $\overrightarrow{M2}$ increases, and can thus be used, in principle, to distinguish goal-related processing from movement-related processing (see also Quaia *et al.*, 2010). It is important to note that $(\overrightarrow{M2'})$ describes the same vector as $\overrightarrow{M2}$ but is directed from the current fixation spot and represents the future or prospective motor plan $(\overrightarrow{M2'})$. By tracking the endpoints of midway saccades before and after saccade adaptation we tested whether midway saccades represent the interaction of $\overrightarrow{M1}$ and $\overrightarrow{M2'}$ or $\overrightarrow{G1}$ and $\overrightarrow{G2}$.

Double-step adaptation task: dissociation of goal and motor vectors

On every step trial of the adaptation block, the second target location was shifted to the right of its old location just after the second saccade to it was initiated. On these initial trials, the eye landed close to the old location of the final target. However, over trials, the subjects

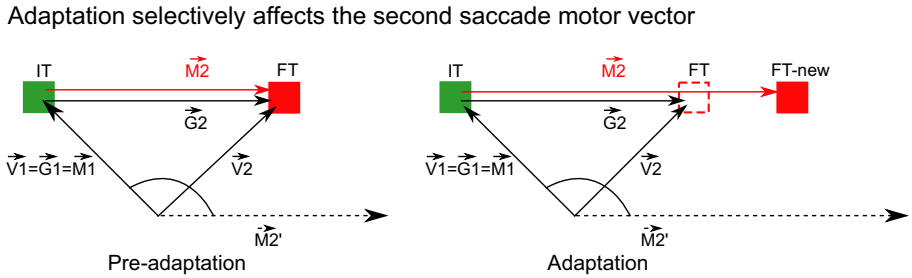

FIG. 3. Dissociation of goal and motor vectors due to saccade adaptation. When subjects are asked to execute a sequence of two saccades programmed in parallel, a first saccade from the fixation point (FP) to the initial target (IT) is followed by a second saccade to the final target (FT) from the IT. Vectors $\overrightarrow{V1}$ and $\overrightarrow{V2}$ describe the location of targets on the retina. Vectors $\overrightarrow{G1}$ and $\overrightarrow{G2}$ describe the location of behaviourally relevant goals. Vectors $\overrightarrow{M1}$ and $\overrightarrow{M2}$ describe the amplitude and direction of two saccades. Vector $\overrightarrow{M2'}$ represents a hypothetical saccade with the same amplitude and direction as $\overrightarrow{M2}$, but aimed directly from the FP. If the motor vectors of two sequential saccades are interacting in parallel, saccade adaptation, should produce a change in the second saccade motor vector $\overrightarrow{M2}$ only, without affecting the goal representation $\overrightarrow{G2}$.

produced second saccades with larger amplitudes (mean ± SEM = 18.11 ± 0.35°) compared to that in the pre-adaptation block (14.25 ± 0.26°; Fig. 4a). This increase in the amplitude of second saccades following adaptation was significant (paired *t*-test $P < 0.001$; $t_{stat} = 12.671$; df = 7). However, there was no effect of adaptation on both the amplitude (paired *t*-test $P = 0.571$; tstat = 0.594; df = 7) and direction (Wilcoxon ranksum test $P = 0.169$; ranksum value = 54.5) of no-step saccades to the location of the second target (Fig. 4b). The mean amplitude and mean direction of no-step saccades to the location of FT in the pre-adaptation block was 11.88 ± 0.16° and 44.47 ± 0.31°, respectively. In the adaptation block, no-step saccades to the second target location were produced with a mean amplitude and mean direction of 11.71 ± 0.28° and 44.79 ± 0.14°, respectively. In the context of the schematic shown in Fig. 3, the above results indicate that only the motor vector ($\overrightarrow{M2_a}$) for the second saccade was adapted, whereas the goal vector for the second saccade ($\overrightarrow{G2}$) was not affected as a result of the target shift.

Parallel programming of motor vectors of sequential saccades in the double-step adaptation task

Parallel programming of sequential saccades during the adaptation task was tested by comparing the endpoint scatter of second saccades in the adaptation block, for different reprocessing time (RPT) intervals. Since saccade reaction times are stochastic, even with a fixed target step delay of ~16 ms, variable RPTs were produced. We divided the individual step trials into low and high RPT groups. If the second saccade was not concurrently planned during the RPT, then for both the RPT bins the endpoints of the second saccades should be similar. On the other hand, if some aspect of the second saccade was processed in parallel with the first saccade plan, second saccade endpoints should be closer to the old location of the second target, especially at the higher RPTs.

As seen in Fig. 4c, at lower RPTs, second saccade endpoints were relatively closer to the location of the final target after the shift (FT-new; 21.10 ± 0.31°). At higher RPTs, however, second saccades' endpoints were closer to the old location of the final target (FT; 17.71 ± 0.44). This difference in the amplitude of second saccades for lower and higher RPTs was significant (paired t-test, $P < 0.001$; tstat = 12.023; df = 7), suggesting that saccades in the adaptation task were planned concurrently. However, in and of itself, it does not explicitly show that the second adapted motor vector was simultaneously planned with the first saccade. To test this, we assessed the pattern of midway saccades, a well-documented behavioural outcome of parallel programming (see Bhutani *et al.*, 2012, 2013).

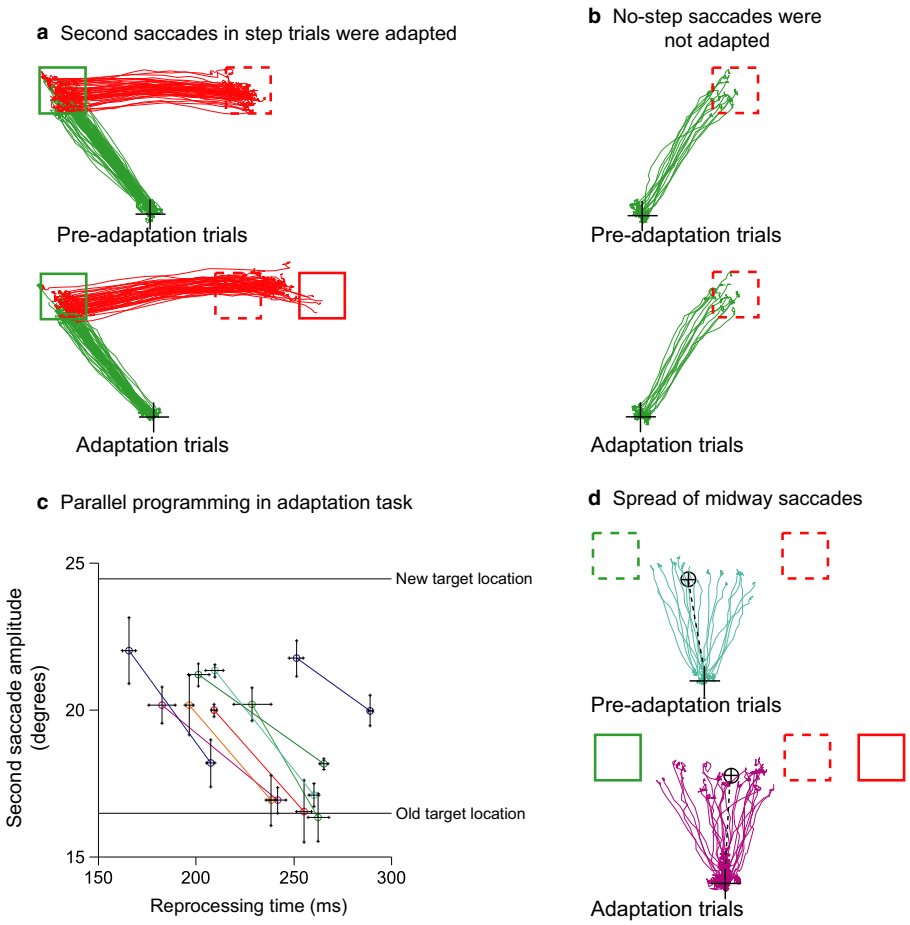

FIG. 4. Adaptation of the second saccade motor vector. (a) Amplitudes of second saccades increased following adaptation. In the pre-adaptation condition, second saccade endpoints were centred on the final target (FT; red dash square). However, following adaptation, second saccades landed closer to the shifted final target (FT-new; red solid square). (b) No difference in the endpoint scatter of no-step saccades to the FT location were seen between pre-adaptation and adaptation blocks. (c) Plot of the mean endpoint location of second saccades in the adaptation block vs. the reprocessing time (RPT) colour coded for each subject. (d) Scatter of midway saccades in step trials is plotted for a representative subject in the pre-adaptation (left) and adaptation blocks (right). Black circles with plus represent the medians of the scatter of midway saccade endpoints and the black line represents the corresponding vector from the initial fixation point (plus sign). The red dashed square is the old location of the final target FT; the red solid square represents the location of the shifted FT (FT-new); the green square represents the IT.

Double-step adaptation task: midway saccades due to the interaction of motor vectors

The adaptation paradigm allowed us to discern whether the adapted motor vector contributed to midway saccades. If the adapted motor vector ($\overrightarrow{M2_a}$) was being planned in parallel with the first motor vector ($\overrightarrow{M1}$), then the endpoint scatter of midway saccades in the adaptation block is expected to shift towards the final position of the second target relative to the midway saccades in the pre-adaptation block. In contrast, in the absence of a shift, midway saccades are likely to be the consequence of an interaction between the two goal vectors, $\overrightarrow{G1}$ and $\overrightarrow{G2}$ with increasing RPT. We found evidence for the former hypothesis.

Figure 4d plots the endpoint scatter of midway saccades in the pre-adaptation (cyan) and adaptation (magenta) blocks for a representative subject. The direction of endpoint scatter of the midway saccades shifted rightwards (two sample Kolmogorov-Smirnov test for distribution, $P = 0.021$, kstat = 0.327). Furthermore, we calculated the cumulative distribution functions (CDF) for the direction of midway saccades to obtain the probability with which saccades landed closer to the IT or to the FT. CDFs were normalized such that the probability of landing closer to the final red target was set as 1 and the probability of landing near the initial target was set as 0. The rightward shift following adaptation was also captured by plotting the cumulative distribution for the direction of midway saccades for pre-adaptation (cyan) and adaptation (magenta) blocks. For every subject there was a significant rightward shift of the CDF ($P < 0.05$) (Fig. 5 and Table 2). To further confirm the rightward shift in the scatter of midway saccades towards the final target, we quantified the direction at the median of the CDF in the pre-adaptation (Pre-adapt$_{0.5}$) and adaptation (Adapt$_{0.5}$) blocks. For the pre-adaptation condition, the median direction of midway saccades was 99.58 ± 2.04° and for the adaptation block the Adapt$_{0.5}$ value was 81.61 ± 1.74°. This shift was significant (paired *t*-test $P < 0.001$; tstat = 15.617; df = 7). Furthermore, we wanted to ensure that this rightward shift in the endpoint scatter of midway saccades following adaptation was not a consequence of a change in their underlying RPTs. To test this, we compared the distribution of RPTs in the pre-adaptation and the adaptation blocks and found no significant difference in the RPT distribution (Kolmogorov-Smirnov test population mean $P = 0.226$; min = 0.08, max=0.54).

Different eccentricity task: parallel programming of sequential saccades

Short intersaccade intervals (ISIs), defined as the duration between the end of the first saccade and the onset of the second saccade, have been considered to be a marker for concurrent processing. We tested for the parallel planning of sequential saccades by plotting the intersaccade interval (ISI), vs. the reprocessing time (RPT). Reprocessing time is the time between the onset of first saccade and the appearance of the second target and is the time available for parallel programming. It refers to the time available to the saccade processing centres to process the second saccade, while the first saccade plan is still underway. The principle for using the ISI vs. RPT plot as a signature of concurrent processing is as follows: if saccades are planned in parallel, then higher RPTs will allow greater time for the processing of second saccade, while the first is still being processed; in turn the second saccade will be generated quickly after the end of first saccade. Thus, intersaccade interval (ISI) should decrease with increase RPT. However, if sequential saccades are planned one after the other, the intersaccade interval (ISI) should not change with RPT.

ISIs and RPTs were computed for each step trial with sequential saccades. Only step trials with ISIs less than the 95th percentile of no-step saccade latencies were used since ISIs greater than the normal saccade latency were likely to have been produced as a consequence of serial processing. Despite individual variability, a decreasing trend in ISIs with increasing RPTs was observed, on

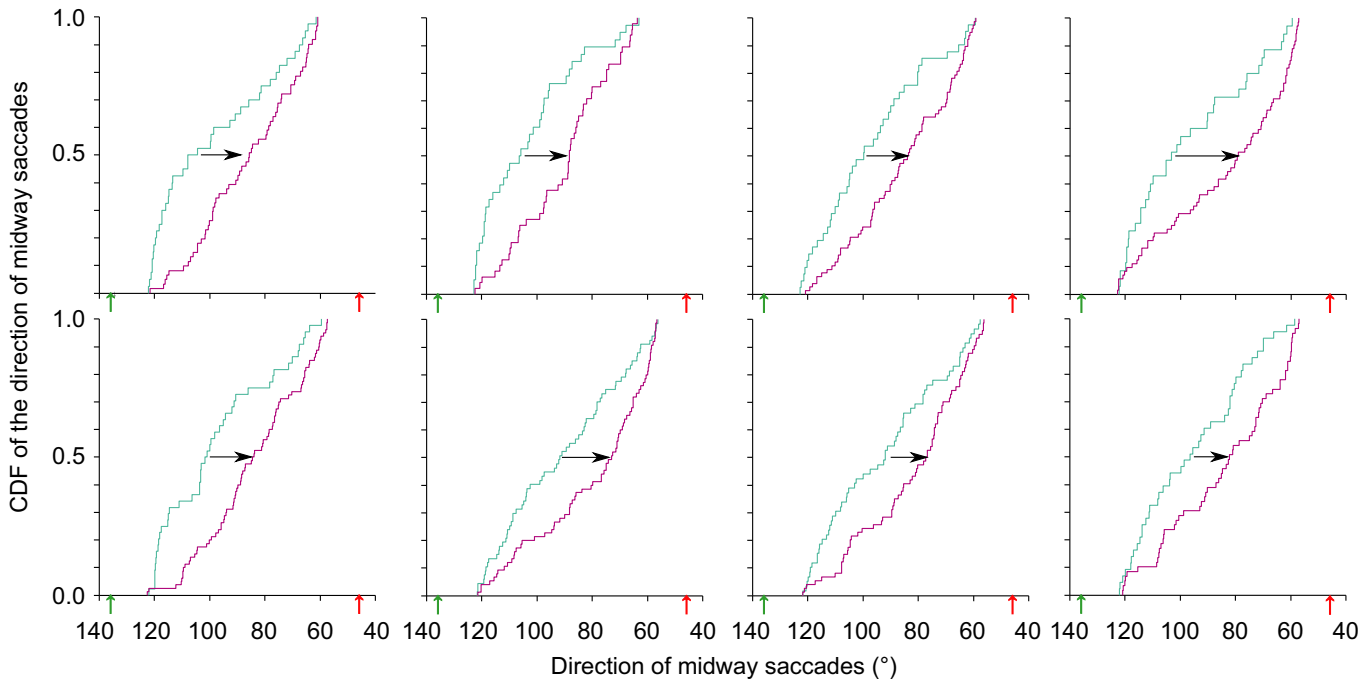

FIG. 5. Cumulative distribution of the scatter of the direction of midway saccades for pre-adaptation (cyan) and adaptation (magenta) blocks for each subject. The *x*-axis has been reversed to show the rightward shift in the scatter following adaptation. Green and red arrows mark the location of IT (135°) and FT (45°).

TABLE 2. *P*-values for the Kolmogorov-Smirnov (KS) test for the difference in the distribution of midway saccades in the pre-adaptation and adaptation blocks. The KS test statistic for each subject is mentioned in brackets

Subject	*P* value
AR	0.0211 (0.327)
JA	0.0037 (0.331)
NI	0.0133 (0.297)
NP	0.0349 (0.244)
NT	<0.0001 (0.402)
PS	0.0034 (0.298)
SD	0.0108 (0.268)
ST	0.0416 (0.267)

average (Fig. 6a). For the population, ISIs typically decreased from ~286 ms to ~109 ms and ~278 ms to ~104 ms, with increasing RPT for the same and different eccentricity conditions, respectively. At larger RPTs the decrease in ISI is much less and typically saturates at RPTs >150 ms. Nonetheless, the average parallel processing rate of the second saccade across the population, as quantified by the best fit line, was −0.61 (±0.04) and −0.58 (±0.03) for the same and different eccentricity conditions, respectively, and is in agreement with the previous results (Becker & Jürgens, 1979; McPeek *et al.*, 2000; Ray *et al.*, 2004).

Collicular Vector Addition (VAd) between two motor plans predict the spatiotemporal pattern of saccade averaging

We used a collicular vector addition model (*VAd*) to predict the endpoint scatter of midway saccades in step trials as a function of the reprocessing time (RPT). Since the FOLLOW task requires the execution of two saccades sequentially, the first saccade vector was always fully represented. However, the endpoint of the initial saccade motor vector was expected to be affected only by the degree of the second saccade processing that occurred in parallel during the reprocessing time (RPT), whereas the first saccade is still in pipeline. Thus, only the second goal or motor vector was weighted such that:

$$w2 = \frac{\mathrm{RPT_{sim}}}{\mathrm{RT_{GO1}}} \tag{9}$$

On the basis of the premise that midway saccades reflect an interaction between two parallel planned linear accumulators (LATER model; see methods for details), we tested whether midway saccades are generated as a consequence of the vector addition (VAd) of the parallel planned motor vectors using the following equation:

$$\mathrm{VAd_{motor}}(H,V) = \overrightarrow{M1} + w2\overrightarrow{M2} \tag{10}$$

Model predictions were tested by comparing the endpoint scatter of initial saccades in step trials in the same and different eccentricity conditions. The endpoint scatter was calculated as follows: the direction (Φ) of each saccade was computed from the inverse tangent of the line segment joining the start and end of the saccade, whereas the amplitude (R) was given by the length of this line segment. Furthermore, the Initial Target (IT) (Ix, Iy), Final Target (FT) (Fx, Fy) and saccade trajectory [H(t), V(t)] were rotated along the Fixation Point (FP) such that the new IT was always vertically up at the 90° position with respect to the FP, whereas the FT was always 45° clockwise to the IT. This transformation allowed us to collate the data across different target step configurations. The horizontal (H_{end}) and vertical (V_{end}) components of these saccades were calculated as:

$$H_{\mathrm{end}} = \mathrm{R}\cos(\Phi) \tag{11}$$

$$V_{\mathrm{end}} = \mathrm{R}\sin(\Phi) \tag{12}$$

They were grouped into ten RPT bins ranging from the shortest to the longest RPTs.

Figure 6b plots the predictions of the $\mathrm{VAd_{motor}}$ model (mean ± SEM for initial saccade endpoints in different RPT bins for a representative subject), for the same and different eccentricity trial conditions, in which the second target was either of the same (12°) or lesser (6°) eccentricity condition, respectively. The simulated values of reprocessing time ($\mathrm{RPT_{sim}}$) were divided into 10 bins and the corresponding mean scatter of the predicted endpoints was obtained. The model predicted that the first saccade endpoints lie closer to IT at shorter $\mathrm{RPT_{sim}}$ conditions and shift away from IT with increasing $\mathrm{RPT_{sim}}$. Since only $\overrightarrow{M2'}$ was weighted, with increasing $\mathrm{RPT_{sim}}$ the contribution of $\overrightarrow{M2'}$ increased, resulting in predicted saccades with amplitudes increasing with $\mathrm{RPT_{sim}}$. As shown in the figures, at short RPTs, saccades were aimed closer to IT, whereas at the longest RPTs, saccades were aimed closer to FT. In between, there was a gradual shift in the saccade endpoint scatter from IT towards FT.

This result suggests that at lower RPTs, when parallel programming of the second saccade is limited, the endpoint of the first saccade is least affected by the planning of the second saccade. With increasing RPT, the influence of the second saccade plan increased gradually, thus shifting the endpoint more towards FT. This shift in the endpoint scatter away from IT and towards FT was significant for both the same eccentricity (one-way ANOVA $P < 0.001$; $F_{9,70} = 41.98$) and the different eccentricity (Kruskal–Wallis $P < 0.001$; χ^2 (9, 70)= 65.48) conditions.

To further assess the ability of the motor addition model to fit the data, we compared the slope of the path for the predicted and observed endpoint scatter with increasing RPT. The mean (±SEM) slope of the observed path for all eight subjects in the same and different target eccentricity conditions were -0.47 ± 0.06 and -2.1 ± 0.39, respectively. The $\mathrm{VAd_{motor}}$ predicted the scatter with slopes of −0.41 and −1.83 for the same and different eccentricity conditions, respectively, where the predicted data points followed the path joining IT and FT and were not significantly different from the observed data (same eccentricity condition, Mann–Whitney U-test $P = 0.08$; different eccentricity condition, Mann–Whitney U-test $P = 0.40$). The values of R^2 for each subject for the $\mathrm{VAd_{motor}}$ model for the two eccentricity conditions are tabulated in Table 3. Overall, the $\mathrm{VAd_{motor}}$ model could predict the endpoint scatter with an overall R^2 value of 0.65 (± 0.09) and could reasonably predict the scatter for 13/16 conditions.

Vector averaging ($\mathrm{VAg_{sensory}}$) model

To contrast the performance of the motor addition model, we also tested the well-known vector averaging model that hypothesizes an interaction between sensory representations ($\overrightarrow{V1}$ and $\overrightarrow{V2}$ in Fig. 3) underlies midway saccades. Averaging was instantiated by weighting both saccades vectors such that the sum of the weights added to unity.

$$w1 = 1 - w2 \tag{13}$$

$$\mathrm{VAg_{sensory}} = \frac{\left(w1\overrightarrow{V1} + w2\overrightarrow{V2}\right)}{w1 + w2} \tag{14}$$

Equation (14) performs the weighted vector averaging of sensory vectors in visual space. As before, model simulations of endpoint

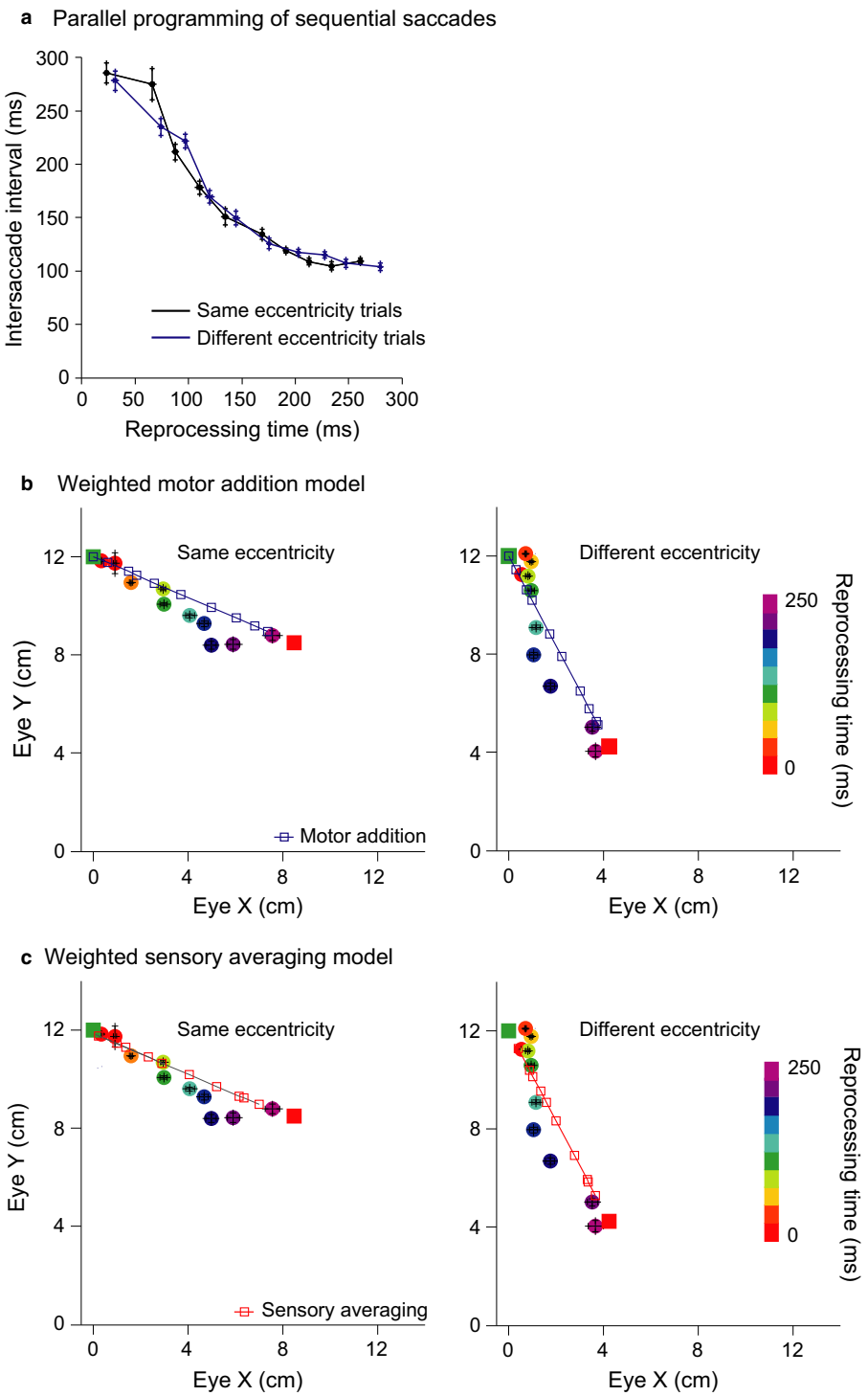

FIG. 6. Saccade averaging due to the weighted addition of motor vectors. (a) Plot of the mean intersaccade interval (ISI) and the reprocessing time (RPT) for the population of subjects who performed the different eccentricity task. (b) Mean ± SEM of observed endpoint scatter as a function of RPT are plotted for an individual subject in the same (left column) and different eccentricity (right column) step trials. At lower RPTs, saccade endpoints land near the IT but shift towards the FT with increasing RPT (filled circles colour coded). RPT-weighted addition of the motor vectors (blue squares; top row) predicts that the endpoint scatter shifts from IT to FT on a path joining the IT and FT, as observed in the data (filled circles colour coded by RPT). The model predictions for sensory averaging (red squares; bottom row) are shown in (c). Green and red filled squares represent the initial target (IT) and final target (FT) locations.

scatter were generated for the models as a function of RPT. Figure 6c plots the predictions of the $VAg_{sensory}$ model for both the same and different target eccentricity conditions. The model predictions were compared with the observed endpoint scatter as a function of RPT. To reiterate, the VAd_{motor} model predicted that the endpoint scatter of saccades would lie on a line joining the IT and FT; similarly, the $VAg_{sensory}$ model also predicted that the saccade end-points would lie on a line joining the IT and FT and was an equally good predictor of the data in comparison with the VAd_{motor} model, and predicted the observed data well with an R^2 value of

TABLE 3. R^2 values for the weighted motor vector addition (VAd_{motor}) model for individual subjects in the different eccentricity task are compared with the R^2 values for the weighted sensory averaging model ($VAg_{sensory}$).

Target configuration	VAd_{motor}	$VAg_{sensory}$
Same eccentricity	0.831	0.898
	0.953	0.906
	0.959	0.949
	0.554	0.713
	0.478	0.834
	0.0000	0.0000
	0.869	0.867
	0.904	0.843
Different eccentricity	0.810	0.818
	0.918	0.883
	0.811	0.705
	0.949	0.4007
	0.000	0.5887
	0.000	0.0000
	0.863	0.704
	0.566	0.166

0.64 (±0.08). Thus, taken together, the motor addition model performed just as well as the sensory averaging model.

Discussion

In this study, the pattern of saccade averaging in a visually-guided double-step adaptation task was used to reveal the computation underlying the parallel programming of the second saccade in the sequence. Although a previous study from our work ruled out the role of sensory processing (Bhutani *et al.*, 2012), the study could not distinguish whether saccade averaging was a consequence of the interaction of goal or motor vectors. We have tried to resolve this issue in this study.

Relationship to previous work

The use of midway saccades as a proxy for parallel programming was first described by the so called Amplitude/Angle transition functions (Amp/AngTF) mentioned in the early studies by Aslin & Shea (1987) and Becker & Jürgens (1979) that show a scatter of saccade endpoints with time delay D, which is equivalent to RPT in this study. Using a time-window average model, which assumed that the stimulus is continuously sampled for a fixed period after its presentation, Becker & Jürgens (1979) proposed that the internal representation of target location gradually shifts along the straight line connecting the first and second target locations. Furthermore, they suggested that as the target shifts during this time-window, a weighted average of two actual locations would be specified as the initial target. Thus, the shorter the interstimulus interval, the closer the weighted average would be to the final target position. Despite these earlier attempts, to the best of our knowledge there has not been any systematic attempt to predict the saccade endpoints as a function of RPT to elucidate the nature of interacting saccade vectors.

This study describes the concurrent planning of a current and a future or 'prospective' motor plan (see also Van der Willigen *et al.*, 2011 and Van Gisbergen *et al.*, 1987a for a similar model). Quaia *et al.* (2010) suggested that motor vectors for both the targets with respect to the fixation point are already computed (here represented as the $\overrightarrow{G2}$ vector); once the gaze lands at the location of IT, the motor vector for second saccade from the IT ($\overrightarrow{M2^*}$) is then computed (here represented as the $\overrightarrow{M2}$ vector) by subtracting the vector $\overrightarrow{M1}$ from it. In contrast to Quaia *et al.* (2010), wherein $\overrightarrow{M2^*}$ is computed after the saccade has been made to the initial target, this study shows that the motor vector that will bring the eye from IT to the FT, maybe represented before eye reaches the IT location, and sometimes even before the first saccade has started. This difference in the representations of motor vectors in this study and the study by Quaia *et al.* (2010) may be because of the differences in the two paradigms. Whereas, in this study, the two saccades were being planned in parallel in a highly predictable sequence, in the study by Quaia *et al.* (2010), subjects were clearly instructed to "plan and execute two distinct saccades, sequentially." Following these implications, we propose that the brain has a representation of a future or a 'prospective' motor plan $\left(\overrightarrow{M2'}\right)$, that will eventually bring the gaze from IT to FT, even before eye has reached the IT. Further, the representation of this prospective motor plan in comparison to the goal vector of the second saccade seems more economically efficient since brain does not have to compute the required subsequent motor vector after every eye movement. Van der Willigen *et al.* (2011) have already elaborated on this idea, and through modelling of SC activity and have shown how curved saccades might also be produced as a result of the interaction of the current and future saccade plans.

Parallel representation of goal vs. motor vectors

Although most previous studies have shown that weighted goal averaging produces a pattern that is good in predicting the endpoint scatter (Becker & Jürgens, 1979; Van Opstal & Van Gisbergen, 1989; Walton *et al.*, 2005; Katnani & Gandhi, 2011), we have shown for the first time that the vector addition of two motor vectors produces an equally good prediction. For three reasons, we believe that motor addition could be a more favourable model. *First*, following the adaptation of the second saccade motor vector, the endpoint scatter of initial saccades shifted rightwards. Since the second saccade goal vector was not adapted, this shift isn't due to the interaction of the competing goal vectors. *Second*, the motor model implies that the brain is able to internally transform the goal of second saccade into a motor vector that represents the desired saccade displacement relative to the future fixation point. This prediction is borne out by the well-documented phenomenon, called predictive remapping (Duhamel *et al.*, 1992), which begins even before the saccade is initiated. Such predictive remapping is not only unique to lateral intraparietal (LIP) cortex (Duhamel *et al.*, 1992), but has also been observed in other regions of the oculomotor system, such as the frontal eye fields (FEF; Umeno & Goldberg, 1997) and the SC (Walker *et al.*, 1995). Evidence for a 'prospective' motor plan is also drawn from the idea of attentional pointers (Rolfs *et al.*, 2011). In the Rolfs *et al.* study, subjects were good in discriminating targets that were presented at the remapped location of the second target from the initial fixation point, suggesting that subjects were attending not only to the actual locations of the first and second targets in the sequence, but to a completely different location whose vector from the fixation point was similar to a motor vector for the second saccade from the IT to the FT. Given the close correspondence and equivalence of spatial attention and saccade endpoint (Hoffman & Subramaniam, 1995; Kowler *et al.*, 1995; Deubel & Schneider, 1996), the data of Rolfs *et al.* are what the motor model predicts. *Third*, the motor model is characterized by an interaction that is additive in nature. This is in contrast to the vector averaging model, which is computationally complex as it requires a form of normalization that has not been observed in the motor system. That is why some studies have proposed a vector summation model as an

alternate mechanism (Van Gisbergen *et al.*, 1987b; Goossens & Van Opstal, 2006). Nevertheless, vector summation may not necessarily preclude vector averaging; they both may coexist, operating on motor and visual representations respectively. In this context it is interesting to note that most double-step tasks have emphasized redirecting the saccade to the final target, as opposed to following the targets. Consistent with this view, we have previously shown differences in the types of midway saccades observed across the two double-step conditions (Bhutani *et al.*, 2012).

Adaptation of the motor vector

Although saccadic adaptation, occurs primarily in the motor system (Hopp & Fuchs, 2004; Pélisson *et al.*, 2010), some studies have also found adaptation in the sensory system (Kohn, 2007; Webster, 2011; Chopin & Mamassian, 2012; Bahcall and Kowler, 1999) as well. However, these studies have typically involved perceptual localizations tasks (Bahcall and Kowler, 1999; Awater *et al.*, 2005; Bruno and Morrone, 2007; Collins *et al.*, 2007; Hernandez *et al.*, 2008). Nevertheless, more recently, a similar involvement of sensory representations during saccadic adaptation has been shown specifically for voluntary saccades but not reactive saccades (Cotti *et al.*, 2009). Since the double-step adaptation task in this study involved a standard visumotor mapping, we assume that saccade adaptation primarily influences the motor representations and forms the basis of our interpretation.

Some experimental evidence to support this claim derives from the effect of adaptation on no-step trials. If adaptation reflected a changed association between the location of a target and its internalized goal location, one would have seen a change in the direction and amplitude of no-step saccades that were directed to the location of the second target, since the effects of adaptation on midway saccades is revealed during the first saccade itself. However, no significant difference was found in the endpoint scatter of no-step saccades in the adaptation and pre-adaptation conditions (Fig. 4b). Moreover, we did not see an effect of adaptation on the horizontal component of these no-step saccades as well. There was also no significant difference in the horizontal component of no-step saccades to the second target location in adaptation and pre-adaptation conditions (P value >0.05).

Shortcomings of the model

Although our results support the interaction of concurrently active motor plans in the generation of midway saccades, we noticed deviations of the observed data from the predicted model. Thus, while, the model predicts a straight path for the shift of endpoint scatter from IT to FT with increasing RPT, visual assessment of the observed data suggests that the path curves inside towards the fixation point for intermediated RPTs. Such inward curvature is also evident in the work of Aslin & Shea (1987) and is not captured by the time-window average model of Becker & Jürgens (1979). Although speculative, this departure could be a consequence of nonlinearities that occur during the interaction of two saccade motor plans (Van Gisbergen *et al.*, 1985; Tweed & Vilis, 1990; Crawford *et al.*, 1991; Groh, 2001; Goossens & Van Opstal, 2006). This notwithstanding, Katnani *et al.* (2012) observed that a weighted addition model with saturation also did not explain the endpoint scatter of evoked saccades in dual-microstimulation conditions.

Acknowledgements

This work was supported by grants from the Department of Biotechnology (DBT), a DBT-IISc Partnership grant and an IRHPA grant from the Department of Science and Technology, Government of India. NB was supported by a fellowship from the University Grants Commission (UGC), Government of India. Current address of NB: Département de Neurosciences, Université de Montréal, Montréal, Québec, Canada.

Author contributions

NB and AM designed the research. NB, SS, DB and NGP performed the research. NB analysed the data. NB and AM wrote the paper. All the authors approved the final version of the manuscript.

References

Armstrong, K.M., Fitzgerald, J.K. & Moore, T. (2006) Changes in visual receptive fields with microstimulation of frontal cortex. *Neuron*, **50**, 791–798.

Aslin, R.N. & Shea, S.L. (1987) The amplitude and angle of saccades to double-step target displacements. *Vision. Res.*, **27**, 1925–1942.

Averbeck, B.B., Chafee, M.V., Crowe, D.A. & Georgopoulos, A.P. (2002) Parallel processing of serial movements in prefrontal cortex. *PNAS*, **99**, 13172–13177.

Awater, H., Burr, D., Lappe, M., Morrone, M.C. & Goldberg, M.E. (2005) Effect of saccadic adaptation on localization of visual targets. *J. Neurophysiol.*, **93**, 3605–3614.

Bahcall, D.O. & Kowler, E. (1999) Illusory shifts in visual direction accompany adaptation of saccadic eye movements. *Nature*, **400**, 864–866.

Barone, P. & Joseph, J.P. (1989) Prefrontal cortex and spatial sequencing in macaque monkey. *Exp. Brain Res.*, **78**, 447–464.

Becker, W. & Jürgens, R. (1979) An analysis of the saccadic system by means of a double-step stimuli. *Vision. Res.*, **19**, 967–983.

Bhutani, N., Ray, S. & Murthy, A. (2012) Is saccade averaging determined by visual processing or movement planning? *J. Neurophysiol.*, **108**, 3161–3171.

Bhutani, N., Sureshbabu, R., Farooqui, A.A., Behari, M., Goyal, V. & Murthy, A. (2013) Queuing of concurrent movement plans by basal ganglia. *J. Neurosci.*, **33**, 9985–9997.

Bruce, C.J. & Goldberg, M.E. (1985) Primate frontal eye fields. I. Single neurons discharged before saccades. *J. Neurophysiol.*, **53**, 603–635.

Bruno, A. & Morrone, M.C. (2007) Influence of saccadic adaptation on spatial localization: compression of verbal and pointing reports. *J. Vis.*, **7**, 16.1–16.3.

Carpenter, R.H. & Williams, M.L.L. (1995) Neural computation of log likelihood in control of saccadic eye movements. *Nature*, **377**, 59–62.

Chopin, A. & Mamassian, P. (2012) Predictive properties of visual adaptation. *Curr. Biol.*, **22**, 622–626.

Coëffé, C. & O'Regan, J.K. (1987) Reducing the influence of non-target stimuli on saccade accuracy: predictability and latency effects. *Vision. Res.*, **27**, 227–240.

Collins, T., Vergilino-Perez, D., Beauvillain, C. & Doré-Mazars, K. (2007) Saccadic adaptation depends on object selection: evidence from between- and within-object saccadic eye movements. *Brain Res.*, **1152**, 95–105.

Cotti, J., Panouilleres, M., Munoz, D.P., Vercher, J.L., Pelisson, D. & Guillaume, A. (2009) Adaptation of reactive and voluntary saccades: different patterns of adaptation revealed in the antisaccade task. *J. Physiol.*, **587**, 127–138.

Crawford, J.D., Cadera, W. & Vilis, T. (1991) Generation of torsional and vertical eye position signals by the interstitial nucleus of Cajal. *Science*, **252**, 1551–1553.

Deubel, H. & Schneider, W.X. (1996) Saccade target selection and object recognition: evidence for a common attentional mechanism. *Vision. Res.*, **36**, 1827–1837.

Duhamel, J.R., Colby, C.L. & Goldberg, M.E. (1992) The updating of the representation in visual space in parietal cortex by intended eye movements. *Science*, **255**, 90–92.

Edelman, J.A. & Keller, E.L. (1998) Dependence on target configuration of saccade-related activity in the primate superior colliculus. *J. Neurophysiol.*, **80**, 1407–1426.

Findlay, J.M. (1982) Global visual processing for saccadic eye movements. *Vision. Res.*, **22**, 1033–1045.

Frens, M.A. & Van Opstal, A.J. (1997) Monkey superior colliculus activity during short-term saccadic adaptation. *Brain Res. Bull.*, **43**, 473–483.

Funahashi, S., Inoue, M. & Kubota, K. (1997) Delay period activity in the primate prefrontal cortex encoding multiple spatial positions and their order of presentation. *Behav. Brain Res.*, **84**, 203–223.

Glimcher, P.W. & Sparks, D.L. (1993) Representation of averaging saccades in the superior colliculus of the monkey. *Exp. Brain Res.*, **95**, 429–435.
Goossens, H. & Van Opstal, A.J. (1997) Local feedback signals are not distorted by prior eye movements: evidence from visually evoked double saccades. *J. Neurophysiol.*, **78**, 533–538.
Goossens, H.H. & Van Opstal, A.J. (2006) Dynamic ensemble coding of saccades in the monkey superior colliculus. *J. Neurophysiol.*, **95**, 429–435.
Groh, J.M. (2001) Converting neural signals from place codes to rate codes. *Biol. Cybern.*, **85**, 159–165.
Hernandez, T.D., Levitan, C.A., Banks, M.S. & Schor, C.M. (2008) How does saccade adaptation affect visual perception? *J. Vis.*, **8**, 3.1–3.16.
Histed, M.H., Bonin, V. & Reid, C. (2009) Direct activation of sparse, distributed populations of cortical neurons by electrical microstimulation. *Neuron*, **63**, 508–522.
Hoffman, J.E. & Subramaniam, B. (1995) The role of visual attention in saccadic eye movements. *Percept. Psychophys*, **57**, 787–795.
Hopp, J.J. & Fuchs, A.F. (2004) The characteristics and neuronal substrate of saccadic eye movement plasticity. *Prog. Neurobiol.*, **72**, 27–53.
Katnani, H.A. & Gandhi, N.J. (2011) Order of operations for decoding superior colliculus activity for saccade generation. *J. Neurophysiol.*, **106**, 1250–1259.
Katnani, H.A., Van Opstal, A.J. & Gandhi, N.J. (2012) A test of spatial temporal decoding mechanisms in the superior colliculus. *J. Neurophysiol.*, **107**, 2442–2452.
Keele, S.W. (1968) Movement control in skilled motor performance. *Psychol. Bull.*, **70**, 378–403.
Kohn, A. (2007) Visual adaptation: physiology, mechanisms and functional benefits. *J. Neurophysiol.*, **97**, 3155–3164.
Kowler, E., Anderson, A., Dosher, B. & Blaser, E. (1995) The role of attention in programming of saccades. *Vision. Res.*, **35**, 1897–1916.
Lashley, K.S. (1951) The problem of cerebral behavior. In Jeffress, L.A. (Ed.) *Cerebral Mechanisms in Behavior*. Wiley, New York, pp. 112–136.
Massey, F.J. (1951) The Kolmogorov-Smirnov test for goodness of fit. *J. Am. Stat. Assoc.*, **46**, 68–78.
McPeek, R.M. & Keller, E.L. (2001) Short term priming, concurrent processing, and saccade curvature during a target selection task in the monkey. *Vision. Res.*, **41**, 785–800.
McPeek, R.M., Skavenski, A. & Nakayama, K. (2000) Concurrent processing of saccades in visual search. *Vision. Res.*, **40**, 2499–2516.
Mushiake, H., Saito, N., Sakamoto, K., Itoyama, Y. & Tanji, J. (2006) Activity in the lateral prefrontal cortex reflects multiple steps of future events in action plans. *Neuron*, **50**, 631–641.
Page, M.P. & Norris, D.G. (1998) The primacy model: a new model of immediate serial recall. *Psychol. Rev.*, **105**, 761–781.
Pélisson, D., Alahyane, N., Panouillères, M. & Tilikete, C. (2010) Sensorimotor adaptation of saccadic eye movements. *Neurosci. Biobehav. R.*, **34**, 1103–1120.
Pouget, P., Emeric, E.E., Stuphorn, V., Reis, K. & Schall, J.D. (2005) Chronometry of visual responses in frontal eye fields, supplementary eye fields, and anterior cingulate cortex. *J. Neurophysiol.*, **94**, 2086–2092.
Quaia, C., Joiner, W.M., FitzGibbon, E.J., Optican, L.M. & Smith, M.A. (2010) Eye movement sequence generation in human: motor or goal updating? *J. Vision*, **10**, 1–31.
Ray, S., Schall, J.D. & Murthy, A. (2004) Programming of double-step saccade sequences: modulation by cognitive control. *Vision. Res.*, **44**, 2707–2718.
Reddi, B.A. & Carpenter, R.H. (2000) The influence of urgency on decision time. *Nat. Neurosci.*, **3**, 827–831.
Robinson, D.A. & Fuchs, A.F. (1969) Eye movements evoked by stimulation of frontal eye fields. *J. Neurophysiol.*, **32**, 637–648.
Rolfs, M., Jonikaitis, D., Deubel, H. & Cavanagh, P. (2011) Predictive remapping of attention across eye movements. *Nat. Neurosci.*, **14**, 252–255.
Schiller, P.H. & Sandell, J.H. (1983) Interactions between visually and electrically elicited saccades before and after superior colliculus and frontal eye field ablations in the rhesus monkey. *Exp. Brain Res.*, **49**, 381–392.
Schmolesky, M.T., Wang, Y., Hanes, D.P., Thompson, K.G., Leutgeb, S., Schall, J.D. & Leventhal, A.G. (1998) Signal timing across the macaque visual system. *J. Neurophysiol.*, **79**, 3272–3278.
Sharika, K.M., Ramakrishnan, A. & Murthy, A. (2008) Control of predictive error correction during a saccadic double-step task. *J. Neurohysiol.*, **100**, 2757–2770.
Shen, K. & Paré, M. (2007) Neuronal activity in superior colliculus signals both stimulus identity and saccade goals during visual conjunction search. *J. Vision*, **7**, 15.1–1513.
Thompson, K.G., Hanes, D.P., Bichot, N.P. & Schall, J.D. (1996) Perceptual and motor stages identified in the activity of macaque frontal eye field neurons during visual search. *J. Neurophysiol.*, **76**, 4040–4055.
Tweed, D. & Vilis, T. (1990) The superior colliculus and spatiotemporal translation in the saccadic system. *Neural Netw.*, **3**, 75–86.
Umeno, M.M. & Goldberg, M.E. (1997) Spatial processing in the monkey frontal eye field. I. Predictive visual responses. *J. Neurophysiol.*, **78**, 1373–1383.
Van der Willigen, R.F., Goossens, H.H. & Van Opstal, A.J. (2011) Linearvisuomotor transformations in midbrain superior colliculus control saccadic eye-movements. *J. Integr. Neurosci.*, **10**, 277–301.
Van Gisbergen, J.A., Van Opstal, A.J. & Schoenmakers, J.J. (1985) Experimental test of two models for the generation of oblique saccades. *Exp. Brain Res.*, **57**, 321–336.
Van Gisbergen, J.A., Van Opstal, A.J. & Roerbroek, J.G.H. (1987a) Stimulus-induced modification of saccade trajectories. In O'Regan, J.K. & Levy-Schoen, A. (Eds), *Eye Movements: From Physiology to Cognition*. Elsevier, Amsterdam, pp. 27–36.
Van Gisbergen, J.A., Van Opstal, A.J. & Tax, A.A. (1987b) Collicular ensemble coding of saccades based on vector summation. *Neuroscience*, **21**, 541–555.
Van Opstal, A.J. & Van Gisbergen, J.A. (1989) A nonlinear model for collicular spatial interactions underlying the metrical properties of electrically elicited saccades. *Biol. Cybern.*, **60**, 171–183.
Van Opstal, A.J. & Van Gisbergen, J.A. (1990) Role of monkey superior colliculus in saccade averaging. *Exp. Brain Res.*, **79**, 143–149.
Verwey, W.B. (1995) A forthcoming keypress can be selected while earlier ones are executed. *J. Mot. Behav.*, **27**, 275–284.
Viviani, P. & Swensson, R.G. (1982) Saccadic eye movements to peripherally discriminated visual targets. *J. Exp. Psychol. Hum. Percept. Perform.*, **8**, 113–126.
Walker, M.F., FitzGibbon, E.J. & Goldberg, M.E. (1995) Neurons in the monkey superior colliculus predict the result of impending saccadic eye movements. *J. Neurophysiol.*, **73**, 1988–2003.
Walton, M.M.G., Sparks, D.L. & Gandhi, N.J. (2005) Simulations of saccade curvature by models that place superior colliculus upstream from the feedback loop. *J. Neurophysiol.*, **93**, 2354–2358.
Webster, M.A. (2011) Adaptation and visual coding. *J. Vision*, **11**, 1–23.
Zambarbieri, D., Schmid, R. & Ventre, J. (1987). Saccadic eye movements to predictable visual and auditory targets. In O'Regan, J.K. & Levy-Schoen, A. (Eds), *Eye Movements: From Physiology to Cognition*. Elsevier, Amsterdam, pp. 131–140.